UDC 544.18.053-549.753

Mechanochemical Processes and a Mechanism of Energy Transformation during Single Crystal Indentation

M. V. CHAIKINA

Institute of Solid State Chemistry and Mechanochemistry, Siberian Branch of the Russian Academy of Sciences, Ul. Kutateladze 18, Novosibirsk 630128 (Russia)

E-mail: chaikinam@solid.nsc.ru

Abstract

Using the method of scanning and high-resolution electron microscopy, zones of normal and tangential indentation (NTI) were investigated for lithium apatite, quartz and fluoride single crystals. The textural, structural and phase transformations revealed have been conventionally ascribed to "deformation" and "diffusion" processes of plastic deformation. In NTI zones of single crystals there have been two levels of structural transformations revealed, with a sharp boundary between them, at a stress equal to the theoretical ultimate stress limit (σ_{TSL}). In the top zone of scratches, within the range of stress from the microhardness value H_s up to the σ_{TSL} value the substance undergoes profound structural and phase transformations with the formation of the amorphous state, "paracrystalline", "liquid crystal" and "two-dimensional" nanoparticles. Substance within the zone of scratches represents a model of mechanically activated substance. In the bed of scratches at the stress value lower than σ_{tsl} values, single crystal fragmentation occurs with the formation of blocks and steps, which models the process of grinding. A wave model is proposed for the transformation of input mechanical energy in the indentation process with the specific power density approximately equal to $3 \cdot 10^{11}$ J/(m$^3 \cdot$ s), which is close to the level of bond energy for atoms in the activated NTI zone. Resulting from the excitation of chemical bonds within the activated NTI zone there are phase and structural transformations occurring.

Key words: single crystals, fluoroapatite, quartz, lithium fluoride, indentation, electron microscopy, mechanism of mechanical activation, structural transformations, input energy

INTRODUCTION

Studies in the field of mechanochemical processes (MCP) are presented in monographs and reviews [1–4]; however the question concerning the mechanism of energy transformation under mechanical activation (MA) of solids remains under discussion till now.

During the last years, the processes of plastic deformation and destruction of solids are considered to be as multilevel, resonant and wave models based on non-equilibrium thermodynamics [5–7]. However, the studies on the processes are mainly limited by the destruction of solids [8, 9] under stress which is several orders of magnitude lower in comparison with stress under MA [3].

For the last years, the data concerning the regimes of MA in mills have replenished by novel data on the character and rate of influence in grinding apparatuses and the state of matter under processing within powerful mills [10–13]. According to the calculated data by the authors of model [11] and experimental data [12], all "physical and chemical" effects of mechanochemical reactors are considered to be caused by a short pulse of pressure ($\sigma \sim 10^{10}$–10^{11} dyn/cm^2) with shifting at the size of the contact area $\Delta x \sim 10^{-6}$ cm, the contact time $\tau \sim 10^{-8}$–10^{-9} s, temperature increase up to $\Delta T \sim 10^3$ K in the course of "dry" friction. Authors of these works assume that there is the presence of several channels for stress relaxation in MA; however one of highly important places is ascribed to an increase in the temperature and the formation of the liquid phase.

The authors of [14] basing on the relationships of classical mechanics considered the numerical aspects of energy at the front of the main crack by the example of alkali-haloid

crystal chip. Under dynamic changes of pressure and temperature, at the "head" of a crack there is energy fluctuation occurring, which energy fluctuation could be accompanied by the emission of subnano- and nanosized clustered particles [14]. Basing on the kinetic theory of strength the authors of [15] determined the energy yields of the formation of structural defects and mechanochemical reactions. It was demonstrated that the character of MCP occurrence is determined by the chemical structure of deformed structures, as well as by the presence of excited states those serve as carriers of excess energy released after chemical bond discontinuitying. However, the authors of these works have not determined the parameters of stress and input energy necessary in order to realize MCP.

The purpose of the present work consisted in determining the influence of mechanical stress upon the profundity of structural changes in solids as well as in revealing the mechanism of transforming the input energy in the course of intense dynamic mechanical impact on the character of structure transformation.

The studies were carried out with the use of normal and tangential indentation (NTI) method for single crystals by scratching. The present method is used in sclerometry and excludes imposing temperatures which is observed under activation in powerful mills [16]. Moreover, this method allows one to determine changing in the state of the structure depending on arising stress and input energy level.

The stress arising at the contact between a single crystal with an indenter under NTI (8 GPa) is of the same order of magnitude with the stress in powerful activators (1–5 GPa) [1–4]. The type of mechanical impact "pressure + shift" under scratching is close to the impact such as "shock + friction" in activators, therefore the use of this method for modelling mechanochemical processes is justified to a considerable extent.

EXPERIMENTAL

As the objects of studies in NTI we used naturally occurring single crystals of fluoroapatite and quartz (Slyudyanka deposit, Irkutsk Region) as well as synthetic lithium fluoride single crystals with various types of chemical bonds, structure and hardness. Fluoroapatite and quartz exhibit hexagonal structure and belonging to group $P6_3/m$, lithium fluoride exhibit cubic structure and belongs to group $Fm3m$. Quartz SiO_2 and lithium fluoride LiF are isodesmic and they have the same type of bonds. Fluoroapatite $Ca_{10}(PO_4)_6F_2$ is non-isodesmic, *i.e.* it has different types of chemical bonds.

Scratching different faces in various crystallographic directions of fluoroapatite single crystals, quartz and lithium fluoride was carried out with the help of Vickers diamond pyramid with the angle of 136° using PMT-3 device at a room temperature with the drawing rate amounting to 0.1 cm/s, the indenter loading ranging within 0.005–2 N, in air medium [3]. The infringement of the structure in the NTI zones of single crystals was investigated with a Jeol JSM-6460LV scanning electron microscope. For studying the state of structural failure with the resolution of a lattice the substance from the top part of scratches was taken, then it was put on punched carbon substrates and further it was investigated with a JEM 2010 electron microscope [17].

Average values of mechanical stress on the surface of contact between a crystal with and indenter were by convention set to be equal to the value of microhardness from sclerometry for given NTI conditions. Microhardness (H_s) was calculated from the formula [18]

$$H_s = 4F/b^2 \quad (1)$$

where F is indentor loading, N; b is scratch width, m.

Table 1 demonstrates microhardness values for apatite obtained under different NTI conditions. Microhardness in NTI for quartz amounts to 7.5–8.5 GPa, lithium fluoride this value ranges within 1–0.98 GPa.

The estimation of stress within the horizontal and vertical sections of scratches was performed according to Hertz theory [19]. This fact has allowed us to determine the character of structural failures depending on arising stress by the example of apatite.

The calculation of average rate of pressure increase (ν_c) under NTI was performed according to the formula

$$\nu_c = H_s/t \quad (2)$$

TABLE 1

Parameters of indentation zones for single apatite crystals under various NTI conditions

Sample No.	NTI system	Indentor loading (F), N	Microhardness (H_s), GPa	Normal stress in crystal/indentor contact zone (σ), GPa	Tangential stress in crystal/indentor contact zone τ, GPa	τ/σ
1	$\{1\bar{2}10\}$					
	[0001]	2	2.96	2.58	1.92	0.7
2	(0001)					
	$<11\bar{2}0>$	1	5.37	4.88	2.15	0.4
3	$\{10\bar{1}0\}$					
	[0001]	1	6.27	3.95	4.83	1.2
4	(0001)					
	$<10\bar{1}0>$	0.5	7.65	5.27	5.60	1.1
5	$\{1\bar{1}22\}$					
	$<11\bar{2}3>$	0.5	8.70	6.09	6.09	1.0
6	(0001)					
	$<10\bar{1}0>$	0.2	7.84	4.38	6.50	1.5
7	(0001)					
	$<10\bar{1}0>$	0.1	15.7	3.77	15.23	4.0

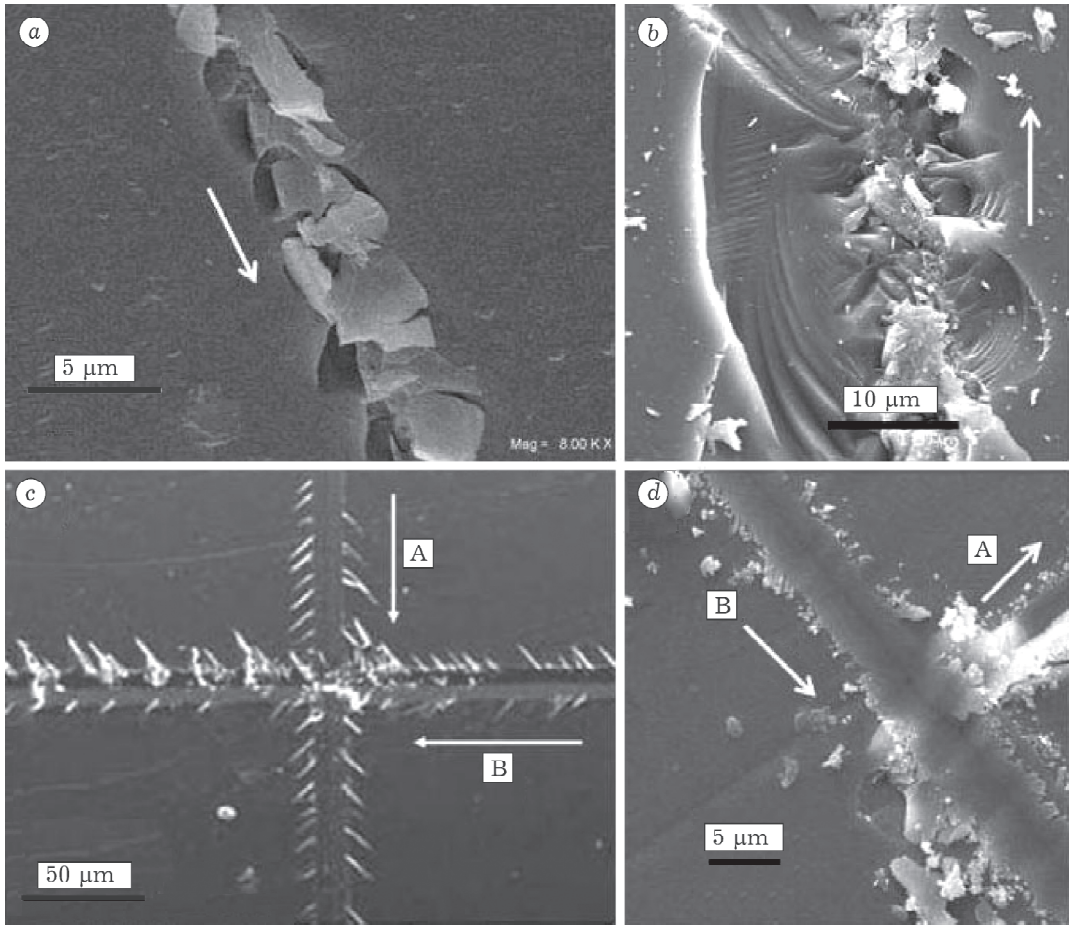

Fig. 1. SEM images of scratches on a single crystal of quartz: *a* – on the basis plane (0001), direction $[11\bar{2}0]$, indentor loading equal to 0.005 N; *b* – on the section at an angle of 20° with respect to the basis plane, loading equal to 0.5 N; *c* – on lithium fluoride single crystal, face (001), direction [100], loading equal to 0.2 N; *d* – on (0001) single crystals of apatite, directions $[11\bar{2}0]$ (A), $[11\bar{2}0]$ (B), loading equal to 0.3 and 0.5 N, respectively.

Here H_s is microhardness, Pa; t is contact time with a single crystal under indenter passing a distance equal the half-width of a scratch, s. The rate of pressure increase was varied from $3.98 \cdot 10^{11}$ to $11.60 \cdot 10^{11}$ Pa/s under the indenter loading equal to 1 and 0.5 N, respectively. Thus, under the conditions of the experiment conducted the NTI of single crystals is a dynamic impact with a high amplitude of pressure, significant rate of pressure increase and considerable gradients of mechanical stress and deformations owing to the subsequent unloading.

RESULTS AND DISCUSSION

Textural and structural transformations within NTI zones

The type of scratches and the texture of substance within NTI zone of quartz, apatite and lithium fluoride single crystals depend on indenter loading, on the face of a crystal and the direction of indentation. The SEM images of scratches on single crystals (Fig. 1) indicate that the scratches on quartz are accompanied by surface infringements with complex structure. At the indenter loading value amounting to 0.005 N in the scratches on the basis plane of quartz the "loosened" substance remains within the bed of scratches (see Fig. 1, *a*). When drawing scratches onto single crystals of quartz on the section at the angle of 20° with respect the basis plane, the particles formed within the zone of contact between the crystal with the indenter are scattering in an explosive manner from the zone of scratches, making the beds of scratches to be open (see Fig. 1, *b*). Within the bed of scratches on quartz, one can observe multiple formation of steps with various shape, whose size amounts to a part of a mi-

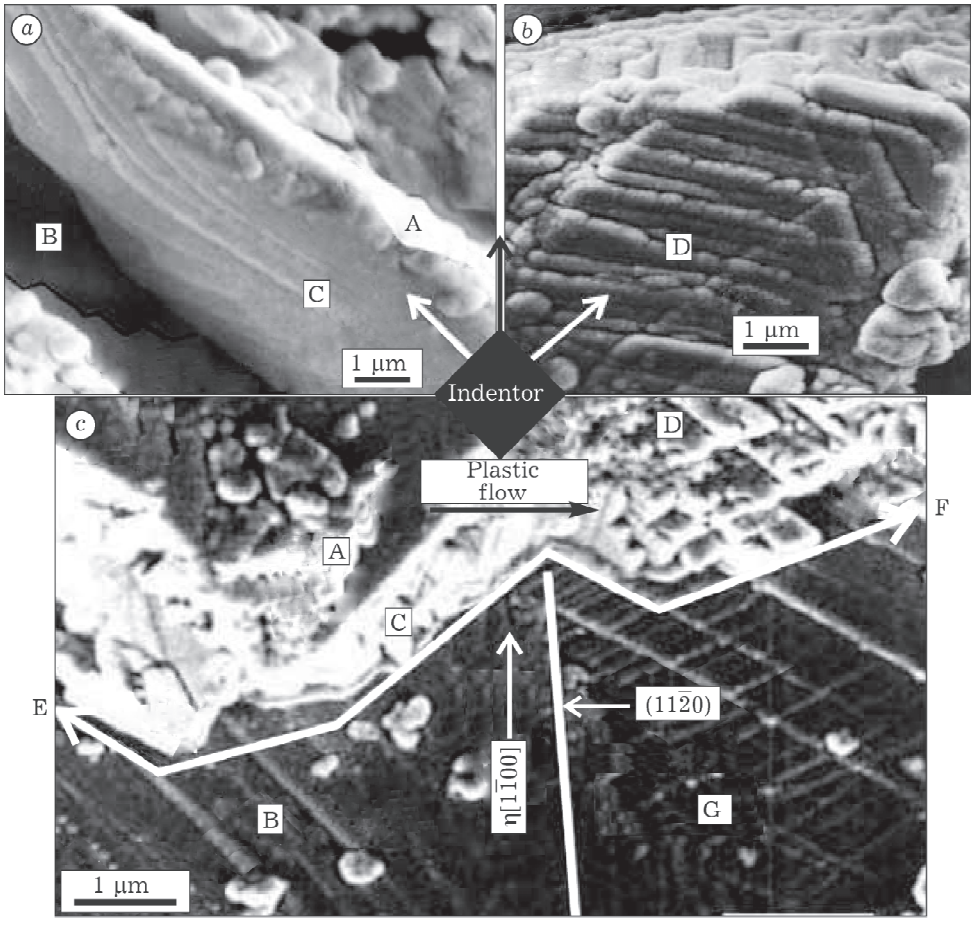

Fig. 2. SEM images of fluoroapatite structural transformations: *a* – disperse structure within the left half of scratch under NTI on (0001), in the direction [11$\bar{2}$0], loading equal to 0.5 N; *b* – blocks with plastic flow within the right half of same scratch; *c* – vertical section of the scratch; A – the surface of contact with indentor, B – steps, C – disperse structure, D – blocks with plastic flow, E–F – the boundary between activation and grinding zones, G – blocks in the grinding zone.

crometer, which indicates complex wave processes under NTI of quartz. Similar "reproduction" of dislocations in the classical literature [20] is designated by the term "grooves". Under NTI of LiF single crystals in the system (001) [100], formation of microcracks has been noted (see Fig. 1, *c*), which, to all appearance, could be caused by the interaction of an ensemble of dislocations and their annihilation with a vacancy sink along planes {110} with respect to the basis. Under indentation of LiF single crystals the author of [21] has revealed an outflow of edge dislocation half-stitches in the same planes. Depending on the indenter loading, under fluoroapatite NTI we observed scratches with the formation either a fragile substance at the edges, or a plastic substance (see Fig. 1, *d*).

Studying the bed of scratches for single crystals of lithium, fluoroapatite and quartz by means of the SEM method has revealed two levels of structural transformation profundity for substance, with a sharp boundary between them, which is distinctly seen by the example of the vertical section of the scratch on apatite (Fig. 2, *c*). According to our estimation, stress on the boundary E–F between two zones calculated according to the Hertz formula [3, 19], amounts to 1.71.8 GPa, which is close to the theoretical ultimate strength limit of apatite σ_{TSL} (1.78 GPa) [3]. Under etching fluoroapatite scratches in 2 % citric acid solution, the substance located higher than boundary E–F was quickly dissolved, and the substance located lower than this boundary was dissolved only along block boundaries.

Hence, the processes occurring in the top part of a scratch could be considered as a model of MA, whereas the bottom part of a scratch where blocks and steps are formed could be considered as a zone of grinding. This fact is rather important for determining the parame-

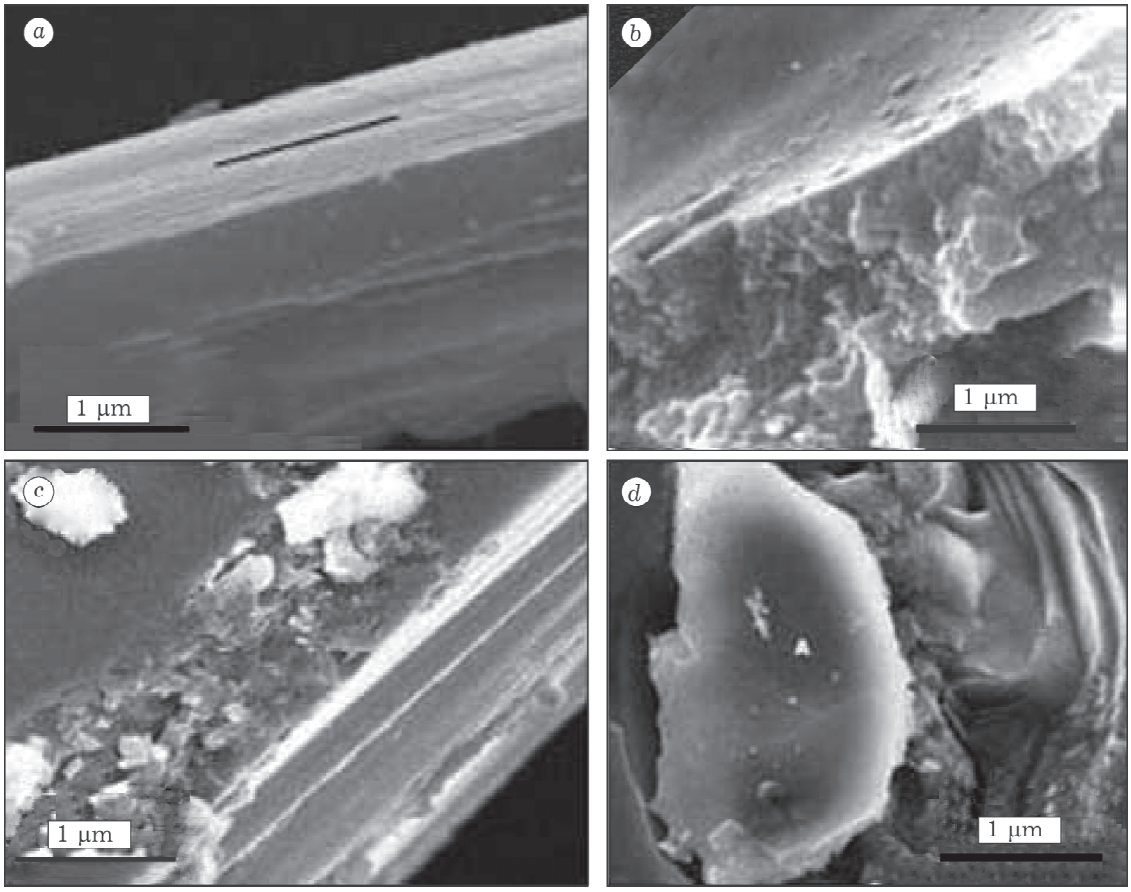

Fig. 3. SEM images of disperse structures (deformation transformation) from the top part of scratches: *a* – lithium fluoride under loading equal to 0.5 N, in the system (001) [100]; *b* – fluoroapatite, in the system (0001) [11$\bar{2}$0], loading equal to 1 N; *c* – quartz, the basis plane in the system (0001) [11$\bar{2}$0], loading equal to 0.5 N; *d* – quartz, single crystal section at an angle of 20° with respect to the basis plane under the indentor loading equal to 0.5 N.

ters of mechanical stress, delimiting the processes of grinding and of mechanical activation. Thus, the MA of substances occurs under arising stress equal to or exceeding the σ_{TSL} value for the solid.

The investigation of MA zone employing the SEM method has demonstrated that monoliths of single crystals after drawing flutes within NTI top area turned into disperse particles in thin nanosized layers (see Figs. 2, *a* and 3). These processes have been conventionally named "deformation" ones. In the case when thin layered plates with the layers of plastic current (see Figs. 2 and 4, *a*) or blocks with plastic current (see Fig. 4, *b*–*d*) are formed, we have conventionally named these processes "diffusion" ones. The character of the structural and phase transformation of substance depends on the crystal face and the direction of indentation.

Within the bed of a single scratch, in the course of indenter drawing owing to application of forces at an angle of 90° (see Fig. 2), there are different processes of plastic deformation sometimes initiated and structural transformations of two types: due to twinning or as the result of interaction of the ensemble of dislocations accompanied with plastic flow (see Fig. 2, *a, b*). As the result of twinning, an ultradisperse layer was formed homogeneous throughout all the half of the scratch (see Fig. 2, *a, c*), lower than its location there are located steps and bands of accommodation in the zone of grinding (see Fig. 2, *a,* G). Figure 2, *c* demonstrates plane $(11\bar{2}0)$ and direction η $[1\bar{1}00]$ of twinning.

Phase transformation of substance with the plastic layers between blocks (see Fig. 2, *b)* is possible under the interaction of the ensemble of dislocations accompanied by the formation clusters of point imperfections [22, 23]. Thus the intensity of plastic flow increases within the centre of the scratch where under the top of the indenter a maximal stress value is observed, and the substance completely turns into "quasiliquid" phase (see Fig. 2, *c*). The dependence of the type of substance transformation on the direction of the imposed forces under indenter movement indicates that the processes in the "activated" NTI zone are also caused by plastic deformation, but at a higher energy level comparing to the zone of grinding.

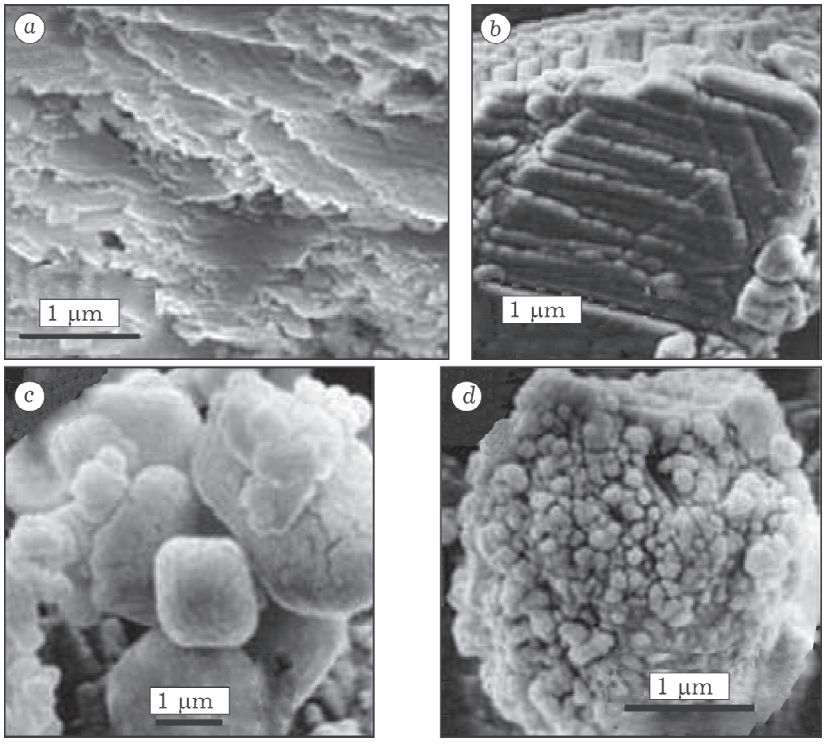

Fig. 4. SEM images of diffusion transformations in the particles from the top area of scratches under loading equal to 0.5 N: *a* – fluoroapatite in the system $(10\bar{1}0)$ $[\bar{1}2\bar{1}0]$; fluoroapatite in the system (0001) $[1\bar{2}10]$; *c*, *d* – quartz in the system $(10\bar{1}0)$ $[\bar{1}2\bar{1}0]$.

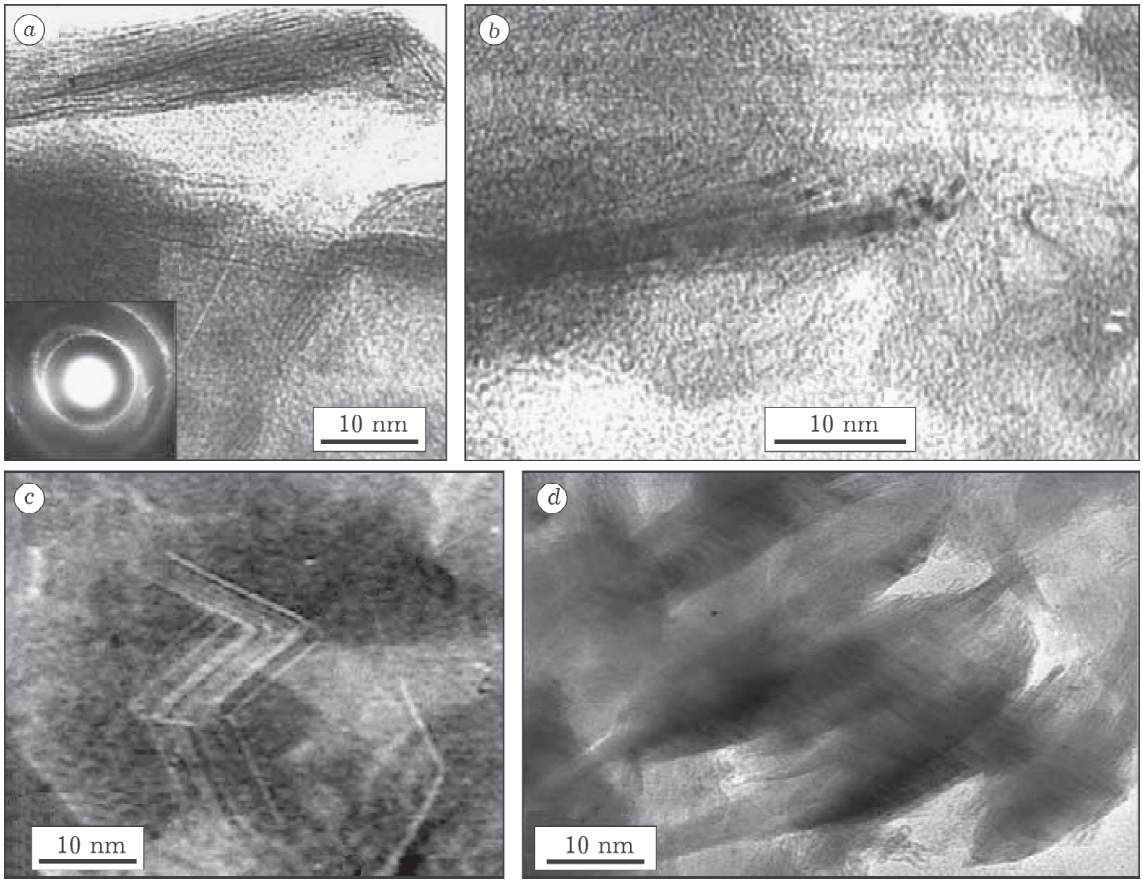

Fig. 5. HRTEM images of deformation transformations of fluoroapatite structure within activated NTI zone in the system (0001) [11$\bar{2}$0] with the indentor, loading equal to 0.5 (*a*), 0.1 (*b*), 0.3 (*c*), 0.2 N (*d*).

The SEM method does not allow one to identify the state of the structure, therefore the substance from the top ("activated") area of scratches was taken and then investigated by means of HRTEM method. According to HTREM data, in the top NTI zone where the arising stress exceeds the value of σ_{TSL} and reaches the values of microhardness (1–8 GPa), owing to the non-uniformity of its distribution there are diverse transformations of structure, phase and even chemical transformations occurring. Figures 5–7 demonstrate HTREM images of the most characteristic types of structural transformations of apatite and quartz. The revealed transformation of the structure within activated NTI zone could also be attributed to the two types such as "deformation" (see Figs. 5, 6) and "diffusion" (see Fig. 7).

The deformation transformations of fluoroapatite structure (see Fig. 5) are accompanied by the formation of "nanoparticles" with stratifying the crystal down to the size of the elementary cell (for the lattice of apatite, parameter $a = 0.936$ nm) (see Fig. 5, *a*, *d*) or shift structures (see Fig. 5, *c*). Characteristic displays of the defectiveness of these particles consist in the disappearance of the lattice parameter along the layer, the compression of the lattice, stratifying, bending and twisting of layers. The layered structure of particles is manifested in the formation of diffraction pictures, inherent in oblique textures such as ellipsoidal rings in electronographic pictures (see Fig. 5, *a*, insert). The deformation transformations could also gradually result in the amorphization of substances (see Fig. 6). As the result of these processes, only fragments in the form of nanoparticle pinholes into the amorphous phase remain from the initial crystal lattice (see Fig. 6, *a*, *c*, *d*). In this case the amorphization of substances, to all appearance, begins from structural infringements of small sites of the extensive lattice (see Fig. 6, *b*).

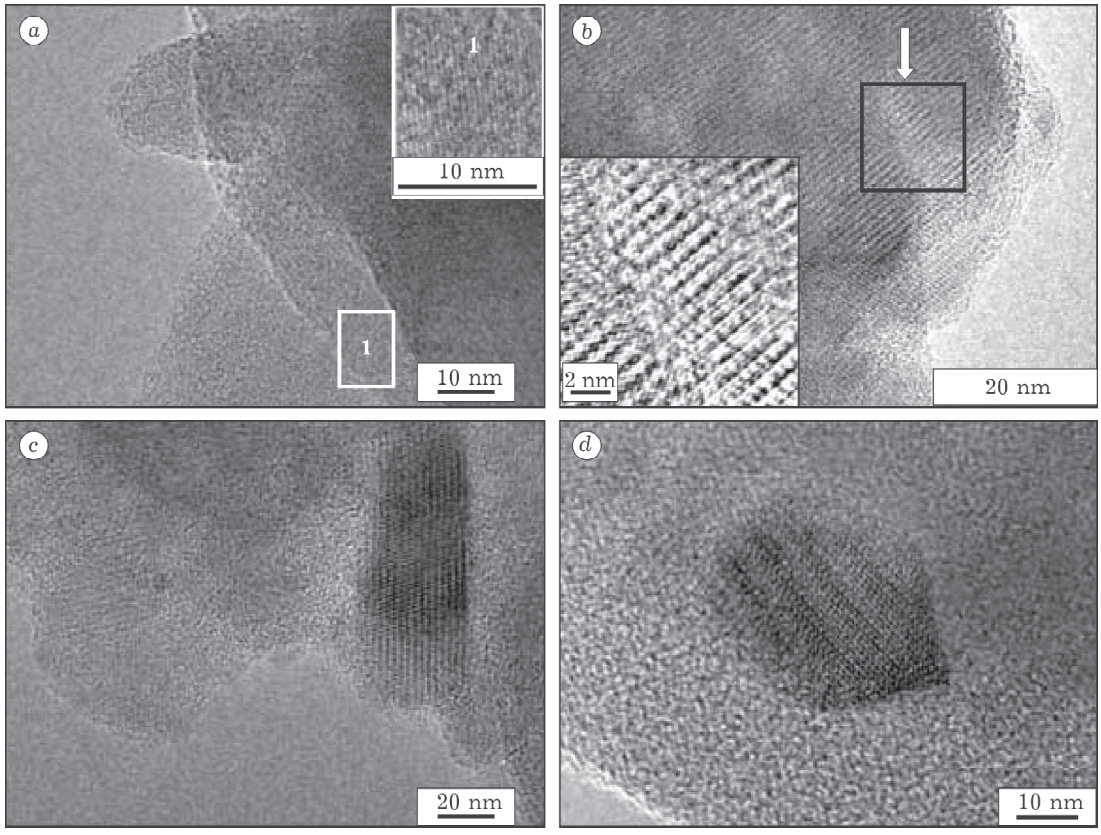

Fig. 6. HRTEM images of activated substance taken from the scratches on quartz (*a*, *c*) and apatite (*b*, *d*) under NTI on (0001) [11$\bar{2}$0] with loading equal to 0.5 N: *a*, *c*, *d* – nanoparticles in an amorphous matrix.

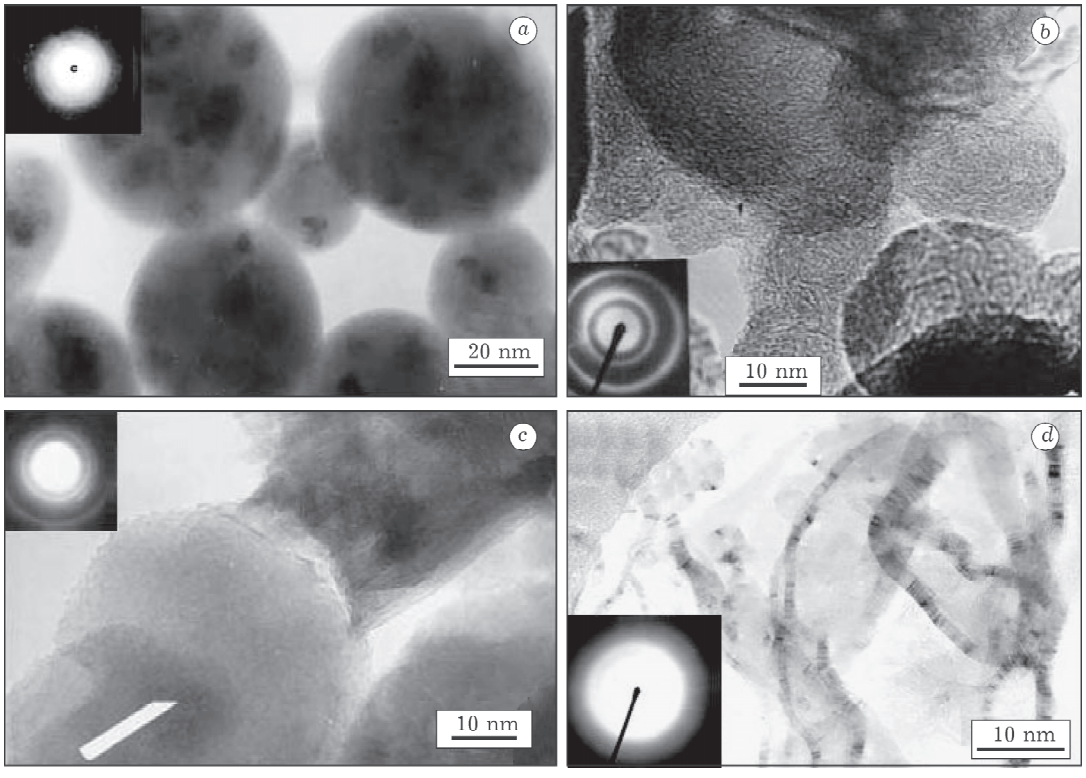

Fig. 7. HRTEM images of activated substance taken from fluoroapatite scratches on the prism face in the system (10$\bar{1}$0) [$\bar{1}$2$\bar{1}$0] (*a*, *b*), and that for quartz on the face in the system (10$\bar{1}$0) [$\bar{1}$2$\bar{1}$0] formed as the result of "diffusion" processes (*c*, *d*).

The diffusion transformations of apatite and quartz structure within the "activated" NTI zone are demonstrated in Fig. 7. The spherical amorphous particles have been formed as the result of crystalline apatite phase transition into the amorphous state in the process of indentation (see Fig. 7, *a*). Similar particles were observed by the SEM method on the surface of contact between single crystal and indenter (see Figs. 2, *a* and 4, *d*), where the substance in the NTI process is in the state of hydrostatic compression at the stress value ranging within 5–8 GPa. In the process of storage, within amorphous particles there are nanocrystals appearing with the interplanar spacing value inherent in β-$Ca_3(PO_4)_2$: d = 0.288, 0.274, 0.160 nm [24] (see Fig. 7, *a*, insert). Basing on this fact one could believe that the process indentation in activated NTI zone results in the decomposition of fluoroapatite according to reaction

$$Ca_{10}(PO_4)_6F_2 \rightarrow 3Ca_3(PO_4)_2 + CaF_2$$

with the formation of a high-temperature form of tricalciumphosphate α-$Ca_3(PO_4)_2$ wherefrom a low-temperature form such as β-$Ca_3(PO_4)_2$ is crystallized in the course of storage. The decomposition of apatite to produce α-$Ca_3(PO_4)_2$ is possible only in a highly excited state of substance equivalent to the temperature of ~2000 K (the temperature of apatite melting and α-$Ca_3(PO_4)_2$ exceeds 1900 K). This process is possible at a high power density of the input energy at the surface of contact, under NTI.

The author of [23] in studying the processes on the surface of friction for solids estimated the energy dissipation basing on specific power density W/V (W is capacity, V is volume) calculated for the contact friction layer according to the formula

$$W/V = \sigma v_s/h \approx 2 \cdot 10^{11}\ \mathrm{J/(m^3 \cdot s)} \quad (3)$$

Here σ is the stress value in the layer of friction, approximately equal to 10 MPa; h is the thickness of the friction layer approximately equal to 5 μm; v_s is the velocity of sifting the surfaces under friction, approximately equal to 0.1 m/s.

Hence, the energy dissipated within this layer during 1 s, exceeds the energy of chemical bond between the atoms in the layer (~10^{11} J/m^3), and the material could be in the excited state, which would result in the substance amorphization and the formation of non-equilibrium phases [23].

Estimating according to expression (3) the specific power density of the energy dissipated on the surface of contact between apatite single crystal and the indenter under NTI, where spherical particles with h ~ 0.5 μm are formed, at the stress value σ ≈ 5 GPa and the velocities of indenter drawing $v_{dr} = 10^{-3}$ m/s we obtain:

$$W/V = \sigma v_{dr}/h \approx 5 \cdot 10^9 \cdot 10^{-3}/(5 \cdot 10^{-7}) \approx \mathrm{J/(m^3 \cdot s)} \quad (4)$$

Thus, the specific power density of the energy dissipated can exceed the energy of interatomic bonding within the layer with the thickness of 0.5 μm (~10^{12} J/m^3). Hence, the decomposition of apatite with the formation of amorphous α-$Ca_3(PO_4)_2$ particles owing to the excited state of the substance at the input power density in the zone of contact with the indenter can be explained to a considerable extent.

"Paracrystlline" [25] structure of of apatite and quartz particles (see Fig. 7, *c*) represents a vortex-like transformation of the initial matrix. This type of particles is somewhat similar to "onion-like" formations of carbon. A low ordering of the structure of "paracrystallineline" particles is confirmed by HRTEM image data (see Fig. 7, *b*, insert) wherein one can distinctly see three halo with the parameters 0.344, 0.303 and 0.117 nm.

Particles of "liquid crystal" type (see Fig. 7, *d*), taken from the scratches on quartz, represent long "elastic" fibres those could be characterized as two-dimensional structures. On the HRTEM image of (0001) zone of these particles (see Fig. 7, *d*, insert) one can see that there is one rather fuzzy reflex of the initial quartz matrix conserved with the parameter d_{0002} = 0.342 nm.

For NTI zone of fluoroapatite single crystal, covering the "activated" part with the thickness $h \approx 5$ μm (see Fig. 2, *a*, *c*), at the stress value equal to σ_{TSL} (~1.8 GPa), and the velocity of indenter drawing $v_{dr} = 10^{-3}$ m/s the specific power density of dissipated energy can be determined as

$$W/V = \sigma v_{dr}/h \approx 1.8 \cdot 10^9 \cdot 10^{-3}/5 \cdot 10^6 \approx 3.6 \cdot 10^{11}\ \mathrm{J/(m^3 \cdot s)} \quad (5)$$

Thus, the specific power density of dissipated energy exceeding the energy of interatomic bonding is inherent in all the "activated" NTI

TABLE 2
Dynamic and energetic parameters of the processes in NTI zone on the contact surface between fluoroapatite single crystal and indentor

Samples	Micro-hardness (H_s), 10^9 Pa	Fluoroapatite density under compression (ρ), ($P = H_s$), 10^3 kg/m^3	Volume of 1 mol of fluoroapatite V_{ap}, 10^4 m^{-3}	Pressure increase rate under NTI (v_p), 10^{-11} Pa/s	Mass velocity jump under NTI (u), m/s	Deformation level (S_{def}), %	Temperature increment due to deformation, (ΔT), K	Specific entropy increment (ΔS_{entr},), J/(mol · K)	Total input energy density (E_t), kJ/mol
Initial	3.12	3.251	–	–	–	–	–	–	–
2	5.37	3.24	3.124	3.98	341	3.9	24.2	115.7	68.1
3	6.27	3.26	3.104	5.02	398	4.5	28.2	133.8	92.0
4	7.05	3.28	3.072	9.56	485	5.5	34.9	166.2	136.8
5	8.7	3.30	3.059	11.6	552	5.9	37.7	178.2	166.8

area when this value accepted to be approximately equal to 10^{11} J/(m^3 · s) [23].

The excited metastable state of atomic system and complex lattice dynamics under NTI could explain the revealed variety of structural transformations, phase and chemical transformations.

The presence of excited states under MCP realization, exceeding atomic vibration levels due to thermal excitation was mentioned more than 30 years ago [26]. The authors of [2] basing on experimental data also demonstrated that the excitation of vibration states arises in the course of tribochemical decomposition, which could be accompanied by electron delocalization and even by ionization. There is no lucidity in the definition of this metastable excited state of matter until now. In early works of German researchers concerning tribochemistry such excited state of matter was named "magma-plasma", it is characterized by short lifetime and accompanied by the damage of structure and overshooting atoms and electrons [27].

The excited state arising at high stress concentration within the local places of the lattice of solids is connected by the authors of [5, 6, 23] with the fact that the energy falling on this volume could be transformed only due to the formation of located dissipative structures. However, the mentioned works are based on the processes occurring in the samples of metals and alloys under stretching up to their destruction, where the stress value is an order of magnitude lower than σ_{TSL} value for the substance. The work [14] devoted to studying the destruction and fractoemission, in the immediate vicinity of a crack "toe" demonstrates the processes under modelling to be similar to the processes we observed on the boundary of "grinding" and "activation" zones under stress equal to σ_{TSL} value for a single crystal.

The issue remains open concerning the mechanism of energy transformation at the moment of influence of imposed forces creating stress higher than the theoretical strength for the solid. The given studies of the NTI zones of single crystals indicate that there is self-organizing system in non-equilibrium state as the result of high pressure amplitudes (5–7 GPa) and the rate of their increase (Table 2). Under considerable amplitudes of pressure the state the solid

at the boundary of compression wave (within the "head" of the wave) and non-perturbed substance can be mathematically described by discontinuous functions of medium parameters [28], *i. e.* such mechanical impact generates strong plastic wave(or conventionally weak "shock" wave) [29]. The author of [7] has demonstrated that in the solid being under the influence of external energy flux, the distribution of deformation wave can occur in the form of shock waves of low intensity.

The jump-like change of the processes accompanied by structural and phase transformations of substance in going from the zone of "grinding" towards the "activated" area under indentation of crystals could be also considered basing on discontinuous vibrations of medium. Let us consider the types of "deformation" and "diffusion" transformations of substance structure observed in the NTI zone (Fig. 8) basing on the wave model. The authors of [30] have described some types of discontinuities. When the components of velocities normal with respect to the surface of discontinuity are equal for non-disturbed (u) and disturbed (u_2) media, there is medium flow through the discontinuity surface, *i. e.* $u = u_2 = 0$, the pressure values P and P_2 on either side of the discontinuity position should be identical. In the case when tangential components of the velocity on either side of the discontinuity position v and v_2 are not equal to each other, the discontinuity is referred to as tangential one (see Fig. 8, zone *C*).

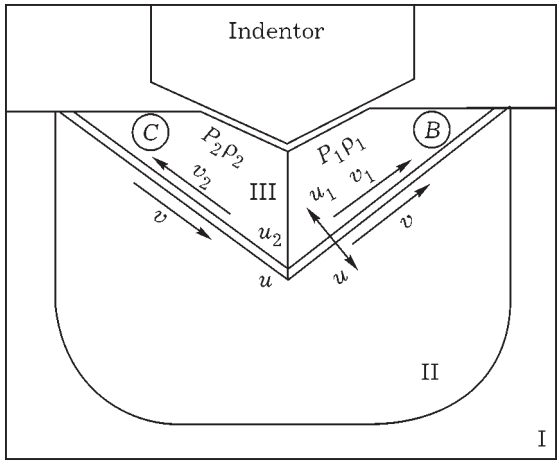

Fig. 8. Scheme of NTI zone for a single crystal: I – plastic zone; II – grinding zone; III – activation zone. A double band in the right part of the field (lower than zone *B*) corresponds generation of a "shock" wave when theoretical ultimate stress limit reached; a double band in the left part (lower than zone *C*) corresponds to the tangential discontinuity; B is activated NTI area with "diffusion" transformations of the structure resulting from the generation, effect of "shock" wave and/or unloading; *C* is "activated" NTI area with "deformation" transformations of structure under the influence of the wave of compression and/or unloading; P_1, P_2 – pressure, ρ_1, ρ_2 – density, u_1, u_2 – normal mass velocity of substance, v_1, v_2 – tangential mass velocity of substance.

When there is a medium flow across the discontinuity surface ($u \neq u_1 \neq 0$), *i. e.* the tangential velocities at the surface of discontinuity are continuous ($v = v_1$) then the pressure, the density and other thermodynamic parameters of the medium state change in a jump-like manner. In this case a "shock" wave takes place (see Fig. 8, zone *C*). Shock waves can be formed only at the stress value exceeding the dynamic limit of fluidity or theoretical ultimate stress limit for the solid [30]. Unloading the substance could propagate as a shock wave, too [28].

Let us compare experimentally observed phase and structural changes of substances on the boundary of grinding and activation zones under NTI of apatite with the types of discontinuity. The first type of discontinuity corresponds to "deformation" processes with the formation of "ultradisperse" layers and nanoparticles (see Figs. 2, *a*, 3, 5 and 6). The following features are inherent therein: 1) the invariance or increase in the density of substance ($\rho_2 = \rho$); 2) identical pressure on either side of discontinuity ($P = P_2$), which is indicated by the uniformity of the activation zone of throughout the width of the scratch (see Fig. 2, *a*); 3) the determining role of shift deformations under cooperative deformational reorganizations of the structure, however it is possible only when $v \neq v_2$.

"Diffusion" transformations of substance correspond to the parameters of medium, undergone the passage of "shock" wave of compression and/or of unloading, which is accompanied by plastic flow (see Figs. 2, *c*, zone D, 4 and 7). In favour of this statement the following data count: 1) the transformation of substance accompanied by intensive plastic flow (see Figs. 2, *c* and 3), *i. e.* the condition $u \neq u_1 \neq 0$ is satisfied; 2) the density of substance ($\rho_1 < \rho$ –

decomposition of apatite with the formation of α-$Ca_3(PO_4)_2$ (see Fig. 7, *a*) decreases; 3) the intensity of "diffusion" processes varies throughout the width of the scratch depending on the stress value (see Fig. 2, *c*, zone D), *i. e.* the pressure varies ($P \neq P_1$).

Thus, the wave model of energy transfer in the MCP in the form of strong plastic deformation waves is in a quite good agreement with the structural phase transformations of substance observed under indentation of single crystals.

According to these representations, by the example of single crystals of apatite, let us estimate dynamic parameters of the processes in the activated zone of indentation. In the course of dynamic impact in the NTI process, under the influence of mechanical momentum Pt the mass of the substance effected by the wave of deformation ρct and referred to the unit of surface area for the section of a sample (in our case – to the surface of contact between a crystal and moving indenter), gets the momentum equal to ρctu. Here from, according to the law of conservation of momentum, we have the following relationship [29]:

$$Pt = \rho cut \quad (6)$$

$$u = P/(c\rho) \quad (7)$$

Here P is pressure; t is pulse time; ρ is the density of initial substance; c is the propagation velocity of compression waves of (local acoustic speed); u is the jump of the mass velocity of substance. It should be noted that according to expression (7), the mass velocity of substance is determined by its pressure and compressibility, this value does not depend on the time of pulse [29]. The mass velocity of substance in the deformation wave under indenting a crystal can be determined as

$$u = P/\rho C_0 \quad (8)$$

Here H_s is the microhardness (provided that $P = H_s$); C_0 is the acoustic speed. For apatite $C_0 = 5.05 \cdot 10^3$ m/s [19], $\rho = 3.15 \cdot 10^{-3}$ kg/m^3. Substituting the corresponding values of H_s for various indentation conditions as well as the above mentioned values of C_0 and ρ, one can determine the jump of the mass velocity of substance according to equation (8). The estimations obtained for the mass velocity of substance within the "activated" zone under NTI of single fluoroapatite crystals change from 341 up to 552 m/s (see Table 2). This value characterizes the propagation velocity for substance excitation within the wave of deformation under NTI.

Let us estimate energy parameters of the processes in NTI zone. Full pressure (P) and energy (E) of the solid can be presented as the sum of elastic P_e and thermal P_t pressure values as well as elastic E_e and thermal E_t energy values, respectively [29]. The change in the balance of forces in the solid depending on external conditions we consider basing on the equations presented below:

$$P = P_e + P_t \quad (9)$$

$$E = E_e + E_t \quad (10)$$

Elastic, or internal, pressure P_e arises as elastic response of a lattice to its all-round compression or expansion. Elastic components P_e and E_e depend on specific volume ($V = 1/\rho$) being equal to full pressure and specific energy at the absolute zero, respectively. The elastic pressure is connected with the potential energy E_e by the relationship [29]

$$P_e = dE_e/dV \quad (11)$$

i. e. the increment of energy is equal to the work of compression. The thermal pressure is connected with the thermal energy E_t *via* the equation

$$P_t = \Gamma_V C_V T/V = \Gamma_V E_t/V \quad (12)$$

Here Γ_V is the Grueneisen coefficient describing the ratio between thermal pressure and thermal energy of lattice; C_V is the heat capacity at constant volume V; T is the temperature. The Grueneisen coefficient Γ_0 at a normal volume of solid V_0 is connected with other parameters of substance by the ratio [29]

$$\Gamma_0 = V_0\alpha/(C_0\chi_0) = \alpha/(\rho_0 C_V \chi) = \alpha C_0^2 / C_V \quad (13)$$

Here χ_0 is isothermal compressibility of substance under normal conditions; α is the coefficient of volumetric thermal expansion; c_0 is the density of substance; C_0 is the acoustic speed determined *via* the compressibility. With a small variation of volume the Grueneisen coefficient Γ can be considered to be equal to its value under normal conditions (Γ_0) [29].

It should be noted that the Grueneisen parameter (Γ, or γ) is one of the major characteristics of crystal lattice, this parameter is included into the state equation, it serves as a measure of anharmonicity of the forces effecting within crystals; this parameter reflects changing these forces under imposing the pres-

sure. With the help of this parameter, one can connect various thermodynamic values. Depending on the system under investigation and problems under solving, several equations were proposed for calculation the Grueneisen coefficient. The authors of [31] proposed the Grueneisen coefficient to be estimated according to the formula

$$\gamma \approx (1 + \mu)/(1 - 2\mu) \quad (14)$$

Here μ is the average Poisson coefficient. The authors of [32] who performed the analysis and comparison of various equations for calculation of the Grueneisen coefficient, inserted a correction A in the equation; its value is calculated also from the values of the Poisson coefficient:

$A = 3/2[(1 - 2\mu)/(2 - 3\mu)]$

In this case the equation (14) can be expressed as it follows:

$$\gamma \approx A[1 + \mu/(1 - 2\mu)] \quad (15)$$

We calculated the Grueneisen coefficient for the estimation of the temperature increase due to the deformation in the course of compression for the contact surface between the crystal and the indentor, and the entropy increment. The estimate for the Grueneisen coefficient according to expression (14) for apatite ($\mu = 0.195$ [3]) has amounted to 1.96. The value close to this one (1.99) has been obtained in calculation according to expression (13), using the data on χ_0 and α from [30, p. 126]. Taking into account the correction A, the Grueneisen coefficient calculated according to expression (15), has decreased down to 1.27. However, these discrepancies are of no basic value for our rough estimates, since the Grueneisen coefficient is used only for an approximate evaluation of a temperature increase and entropy increment resulted from deformation.

Basing on the data concerning the compressibility of fluoroapatite [30, p. 126], the reduction of the volume (see Table 2) and its microhardness value, we have estimated the deformation of fluoroapatite single crystal at the contact with an indenter:

$$S_{\text{def}} = V_0 - V_c/V_0 \quad (16)$$

Here V_c is the volume of 1 mol of fluoroapatite under compression; V_0 is the volume of 1 mol of fluoroapatite in the initial state (see Table 2). The estimate of temperature increase under the conditions of adiabatic relationship between the temperature and volume was performed according the expression

$$T/T_0 = (V_0/V)^{\Gamma} \quad (17)$$

Here T is the temperature within the contact zone under NTI; $T_0 = 298$ K; Γ is the Grueneisen coefficient. The data obtained indicate that the temperature increase resulting from deformation amounts to only several tens of degrees, whereas all the structural and phase fluoroapatite transformations observed occur owing to the intensive wave of plastic deformation as well as its interaction with the lattice.

The estimate of entropy (S) was calculated according to the expression [29]

$$S = C_V \ln T/T_0 (V/V_0)_0^{\Gamma} + S_0 \quad (18)$$

Here S_0 is the entropy value under normal conditions; C_V is the heat capacity at the constant volume, equal to 751.9 J/K [34, Table 1.3]. The first item, the increment of the specific entropy under different conditions of fluoroapatite NTI, varies within range of 115–178 J/(mol · K) (see Table 2), which corresponds to 15–23 % of the specific entropy of fluoroapatite $Ca_{10}(PO_4)_6F_2$ equal to 775 J/(mol · K) at 298.15 K [34, Table 1.3].

Basing on the data concerning the microhardness those we have assumed to be equal to the pressure on the contact surface between fluoroapatite single crystal and the indenter ($P = H_s$), and the compressibility of fluoroapatite at this pressure [33, p. 126] we have performed the estimation of the density of the input specific energy (E_{in}) under NTI [29]:

$$E_{\text{in}} = P(V_0 - V) \quad (19)$$

Here V_0 is the volume of initial substance; V is the volume after compression. The calculation has demonstrated, that the density of the input specific energy within the zone of contact between the crystal and the indenter for different N-TI conditions ranges from 68 to 166 kJ/mol; this value is comparable with the data we had obtained earlier with the use of a calorimetric method (80–122 kJ/mol) for fluoroapatite samples after MA in a planetary type mill [35, 3]. Virtually, it is latent energy which characterizes a nonequilibrium state of mechanically activated substance making its reactivity to increase.

CONCLUSION

The studies concerning NTI zones of fluoroapatite, quartz and lithium fluoride single crystals using SEM and HRTEM methods have

revealed two levels of structure transformation profundity, those depend on mechanical stress arising.

The estimation of stress distribution within vertical sections of scratches on fluoroapatite has demonstrated that the sharp boundary between the zones with different level of structural transformation is formed at the stress values equal to theoretical ultimate stress limit (σ_{TSL}) for the substance.

Within the area of scratches higher than this boundary the substance of single crystals undergoes qualitative changes with the formation of metastable phases in the form of amorphous spherical, *para*-crystalline particles, two-dimensional formations and pinholes of nanoparticles into an amorphous phase. The decomposition of fluoroapatite to give α-$Ca_3(PO_4)_2$ and CaF_2 has been also revealed. This NTI area represents a model for a "mechanically activated substance".

In the bed of scratches, where the stress is less than σ_{TSL} value, the fragmentation of single crystals and the formation of block structures and steps of intricate shape is observed to occur. This NTI area serves as a model of grinding.

The revealed changes in the texture and structure of single crystals within NTI zones have been characterized as "deformation" and "diffusion" transformations those depend on the direction of imposed forces in the course of indentor movement. This indicates the fact that the textural and structural transformations within both zones occur resulting from relaxation processes due to lattice plastic deformation, but at different energy levels. For fluoroapatite we have determined the input specific energy on the contact surface under NTI (68–166 kJ/mol) and the increment of specific entropy (115–178 J/(mol · K)).

A wave model is proposed for the transformation of the input mechanical energy with specific power density (~$3 \cdot 10^{11}$ J/($m^3 \cdot s$)) close to the bonding energy level for atoms close within "activated" NTI zone. Phase and structural transformation are found out resulting from the excitation of chemical bonds in this zone.

Acknowledgement

Author expresses sincere gratitude to the researchers of the Boreskov Institute of Catalysis, SB RAS, V. I. Zaykovskiy and N. A. Rudina for their help in carrying out electron microscopy studies.

REFERENCES

1 E. G. Avvakumov, Mekhanicheskiye Metody Aktivatsii Khimicheskikh Protsessov, Nauka, Novosibirsk, 1986.
2 G. Heinke, Tribochemistry, Akademie-Verlag, Berlin, 1984.
3 M. V. Chaikina, Mekhanokhimiya Prirodnykh i Sinteticheskikh Apatitov, Izd-vo SO RAN, Novosibirsk, 2002.
4 V. V. Boldyrev, *Usp. Khim.*, 5, 3 (2006) 203.
5 V. E. Panin, V. E. Egorushkin, *Fiz. Mezomekhanika*, 11, 2 (2008) 9.
6 V. E. Panin, V. E. Egorushkin, *Fiz. Mezomekhanika*, 12, 4 (2009) 7.
7 F. Mirzade, *Zh. Tekhn. Fiz.*, 72, 10 (2002) 53.
8 M. P. Wnuk, *Fiz. Mezomekhanika*, 12, 4 (2009) 71.
9 O. B. Neimark, Yu. V. Bayandin, V. A. Leontiev *et al.*, *Fiz. Mezomekhanika*, 12, 4 (2009) 47.
10 E. V. Shelekhov, V. V. Therdyntsev, L. Yu. Pustov *et al.*, NATO Science Partnership Sub-series: 3 High Technology (Proceedings), Kluwer Acad. Publ., Dordrecht, 2000, vol. 80, p. 139.
11 F. Kh. Urakaev, V. V. Boldyrev, *Powder Technol.*, 107 (2000) 93.
12 F. Kh. Urakaev, V. V. Boldyrev, *Powder Technol.*, 107 (2000) 197.
13 J. Alkebro, S. Begin-Colin, A. Mocellin and R. Warren, *J. Solid State Chem.*, 164 (2002) 88.
14 F. Kh. Urakaev, I. A. Massalimov, *Fiz. Tv. Tela*, 47, 9 (2005) 1614.
15 O. Yu. Butyagin, A. N. Streletskiy, *Fiz. Tv. Tela*, 47, 5 (2005) 830.
16. Kwon Yong-Soon, K. V. Gerasimov, Yoon Sok-Keel, *J. Alloys Comp.*, 346 (2002) 276.
17 M. V. Chaikina, N. A. Rudina, V. I. Zaikovskii, V Int. Conf. on Mechanochemistry and Mechanical Alloying, INCOME-2006 (Abstracts), Novosibirsk, 2006, p. 108.
18 V. K. Grigorovich, *Zavod, Lab.*, 8 (1958) 1007.
19 N. P. Yushkin, Mekhanicheskiye Svoystva Mineralov, Nauka, Leningrad, 1971.
20 J. Friedel, Dislocations, Pergamon Press, Oxford, 1964.
21 Yu. S. Boyarskaya, Deformirovaniye Kristallov pri Ispytanii na Mikrotverdost', Shtiintsa, Kishinev, 1972.
22 V. V. Rybin, Bolshiye Plasticheskiye Deformatsii i Razrusheniye Metallov, Metallurgiya, Moscow, 1986.
23 V. I. Vladimirov, *Treniye. Iznos. Smazka*, 10, 2 (2008) 7.
24 B. Diskens, L. Shroeder, W. E. Broun, *J. Solid State Chem.*, 10, (1974) 232.
25 J. V. Sanders, J. A. Spink, *J. Appl. Cat.*, 5, 1 (1983) 65.
26 V. V. Boldyrev and G. Heinicke, *Z. Chem.*, 19 (1979) 353.
27 P.-A. Thissen, K. Meyer, G. Heinicke, Grundlagen der Tribochemie, Akademie-Verlag, Berlin, 1967.
28 K. P. Stanyukovich (Ed.), Fizika Vzryva, Nauka, Moscow, 1967.
29 Ya. B. Zeldovich, Yu. P. Raizer, Fizika Udarnykh Voln i Vysokotemperaturnykh Gidrodinamicheskikh Yavleniy, Nauka, Moscow, 1966.
30 G. A. Adadurov, *Usp. Khim.*, 5 (1986) 555.
31 D. S. Sanditov, G. M. Bartenev, Fizicheskiye Svoystva Neuporyadochennykh Struktur, Nauka, Novosibirsk, 1982.
32 D. S. Sanditov, V. V. Mantatov, M. V. Darmaev, B. D. Sanditov, *Zh. Tekhn. Fiz.*, 79, 3 (2009) 59.
33 Spravochnik Fizicheskikh Konstant Gornykh Porod (Handbook), Mir, Moscow, 1969.
34 J. C. Elliott, Structure and Chemistry of Apatites and Other Calcium Orthophosphates, Elsevier, Amsterdam *etc.*, 1994.
35 V. V. Boldyrev, M. V. Chaikina, G. N. Kryukova, *Dokl. AN SSSR*, 286, 6 (1986) 892.